



energies



Article

An Increase in the Energy Efficiency of R744 Heat-Using Thermotransformers

Vyacheslav Arsenyev, Ján Piteľ, Oleksandr Korol, Serhii Sharapov, Jana Mižáková, Ivan Pavlenko and Vitalii Ivanov

Special Issue

Cooling and Heat Exchange Systems

Edited by

Dr. Pascal Clain



<https://doi.org/10.3390/en16217372>

Article

An Increase in the Energy Efficiency of R744 Heat-Using Thermotransformers

Vyacheslav Arsenyev¹, Ján Pitel² , Oleksandr Korol¹, Serhii Sharapov¹ , Jana Mižáková² ,
Ivan Pavlenko^{1,2,*}  and Vitalii Ivanov^{1,2} 

- ¹ Faculty of Technical Systems and Energy Efficient Technologies, Sumy State University, 2, Rymskogo-Korsakova St., 40007 Sumy, Ukraine; v.arsenyev@kttf.sumdu.edu.ua (V.A.); o.korol@kttf.sumdu.edu.ua (O.K.); s.sharapov@kttf.sumdu.edu.ua (S.S.); ivanov@tmvi.sumdu.edu.ua (V.I.)
- ² Faculty of Manufacturing Technologies with a Seat in Prešov, Technical University of Košice, 1, Bayerova St., 080 01 Prešov, Slovakia; jan.pitel@tuke.sk (J.P.); jana.mizakova@tuke.sk (J.M.)
- * Correspondence: i.pavlenko@cm.sumdu.edu.ua

Abstract: This article deals with improving waste heat transformation in heat-using thermotransformers. Based on the directives of the European Commission on refrigeration equipment requirements, the possibility of using carbon dioxide (R744) in heat-using thermotransformers was evaluated. The possibility of the effective use of heat-using thermotransformers operating within the Chistyakov–Plotnikov cycle in the heat pump mode was assessed. As a result, a comparative analysis was performed with existing modern plants for combined cycles with an expander, for the expansion of CO₂ in saturated steam, a suction gas heat exchanger (SGHE), and a compressor–expander unit. The design schemes with a throttling device and an SGHE were selected for a comparative analysis. As a result, calculation models for evaluating the operating parameters for the initial and proposed design schemes were developed. These models allow for evaluating thermodynamic and mode parameters for heat-reducing thermotransformers. They also allow for ensuring energy efficiency indicators and conversion factors for each cycle. Overall, the dependencies for the cycle conversion ratio for the pressure increase stage in the compressor were obtained for various under-recovery rates. Moreover, the cycle conversion ratios for the proposed design schemes were obtained depending on the discharge pressure of the first compressor. The proposed design schemes allow for increasing the energy efficiency of heat-using thermotransformers by an average of 23%, depending on the suction pressure in the compressor.

Keywords: energy efficiency; thermotransformer; carbon dioxide; process innovation; pressure ratio; cycle coefficient of performance



Citation: Arsenyev, V.; Pitel, J.; Korol, O.; Sharapov, S.; Mižáková, J.; Pavlenko, I.; Ivanov, V. An Increase in the Energy Efficiency of R744 Heat-Using Thermotransformers. *Energies* **2023**, *16*, 7372. <https://doi.org/10.3390/en16217372>

Academic Editor: Pascal Clain

Received: 3 October 2023

Revised: 27 October 2023

Accepted: 30 October 2023

Published: 31 October 2023



Copyright: © 2023 by the authors. Licensee MDPI, Basel, Switzerland. This article is an open access article distributed under the terms and conditions of the Creative Commons Attribution (CC BY) license (<https://creativecommons.org/licenses/by/4.0/>).

1. Introduction

At the current stage of development of heat pump technology, the key issues are energy efficiency and environmental safety [1,2]. Due to the need to fulfill international agreements, many traditional refrigerants based on hydrofluorocarbons (HFC) are abandoned to limit the emission of substances that increase the greenhouse effect. Therefore, refrigerants based on natural low-boiling substances are more widely used (e.g., carbon dioxide R744, ammonia R717, and isobutane R600a). One of the refrigerants that can be used in these conditions is CO₂ (R744) since it is safe, non-flammable, not expensive, and widely available on the market.

R744 has advantages over existing analogs, e.g., zero ozone-depleting potential (ODP). Moreover, its global warming potential (GWP) is thousands of times smaller than common refrigerants. Also, CO₂ has several significant thermodynamic properties, including a high heat transfer coefficient, relatively low sensitivity to pressure losses, and relatively low viscosity [3].

Heat-using thermotransformers are heat and cold supply systems based on waste heat transformation. They are widely used in climatic installations. However, international standards, which permanently update refrigerant requirements, require an improvement of the available design schemes. Therefore, process innovation in heat-using thermotransformers and using environmentally friendly and safe refrigerants is an urgent problem. It is necessary to perform a comparative analysis with existing analogs to evaluate the energy efficiency of the refrigerant R744 in such systems.

While heat-using thermotransformers are becoming widespread, a more detailed study of the operating process and improvements to their working cycle are needed [4]. The research works [5,6] considered the possibility of using CO₂ in heat pump systems. However, this creates a problem associated with high condensation and evaporation temperatures, leading to a transcritical cycle. Simultaneously, in articles [7–9], the feasibility of implementing transcritical cycles of heat pump systems on carbon dioxide with a throttle system and an expander system was evaluated [10,11]. The authors note that these types can be implemented in one- or two-stage design schemes. Nevertheless, using a two-stage scheme increases the energy efficiency of the working cycle [12].

Another way to increase the energy efficiency of heat-using thermotransformers is by using combined cycles (i.e., an expansion of CO₂ in the saturated steam region, a regenerative heat exchanger, or a compressor–expander unit) [13]. Notably, the research work [14] stated that the combined cycle with CO₂ expansion in the saturated steam region is used for high-performance installations. Expanding the expansion zone and ensuring the outlet temperature in the saturation region is necessary for its implementation. However, the implementation of a combined cycle with a regenerative heat exchanger is possible if the steam is overheated before the compressor. This process can be implemented in a regenerative heat exchanger with relatively low inlet steam superheating and flow expansion to the saturation mode in the expander. As a result, an insignificant difference in the specific adiabatic work occurs, which allows an acceptable cycle coefficient of performance to be maintained [15].

Simultaneously, the combined cycle with a compressor–expander unit makes it possible to increase the cycle's conversion factor due to an increase in the temperature difference of the medium heated in the secondary circuit. Particularly, the research works [16,17] proposed a heat pump cycle in which expansion with subsequent throttling was implemented.

Also, based on the results of numerical and experimental studies [18–21], it can be concluded that CO₂ use is quite effective in a specific range of pressures and temperatures. On the other hand, a possible way to create an energy-efficient heat-using thermotransformer is to switch to the Chistyakov–Plotnikov cycle [22], combining the abovementioned advantages. Also, the transition from traditional HFC-type refrigerants to natural and safe ones (e.g., R744) additionally increases the environmental safety indicators of the proposed circuit solutions [23,24].

Based on numerical studies of R744-based heat-using thermotransformers for combined cycles with expansion in the saturated steam region and a regenerative heat exchanger and with a compressor–expander unit [25–27], the proposed design schemes can potentially have relatively high energy efficiency indicators. Remarkably, the main difference from the traditional scheme is the development of the cycle of the CO₂-based heat-use thermotransformer in the heat pump mode.

Due to the analysis mentioned above, the following research gaps were identified. Firstly, refrigeration technologies' rapid development requires the permanent development of energy-effective and environmentally friendly refrigerants. Also, chlorine- and HFC-containing compounds should be completely abandoned.

Secondly, the results of recent studies are primarily aimed at finding schematic solutions and the most effective modes of operation of technological systems of heat and cold supply through the implementation of critical cycles. Simultaneously, the possibility of waste heat transformation is almost not considered. However, this also can increase the energy efficiency of R744 heat-using thermotransformers.

This article aims to improve the efficiency of heat-recovery thermotransformers with the R744 working medium, which operates based on the Chistyakov–Plotnikov working cycle. To achieve this goal, the following research objectives were formulated. Firstly, existing installations of heat-using thermotransformers should be analyzed with subsequent selection of the most energy-efficient working cycles. Secondly, the development of an improved design scheme for R744 heat-using thermotransformers should be proposed.

Thirdly, a calculation model for evaluating the thermodynamic and mode parameters of the working cycle should be developed for a heat-using thermotransformer with the refrigerant R744 in heat pump mode. Such a model should allow for evaluating the energy efficiency indicators of the proposed cycle. Finally, the obtained energy efficiency indicators should be analyzed, and practical recommendations to introduce R744 heat-using thermotransformers should be formulated.

Overall, the article evaluates the influence of the overheating of carbon dioxide vapors in front of the compressor on energy efficiency.

2. Materials and Methods

2.1. The Initial Design Schemes

After analyzing the existing design schemes of thermotransformers, two main types can be highlighted. The first (Figure 1) is based on a throttling device (Figure 1), and the second (Figure 2) is with a suction gas heat exchanger (SGHE).

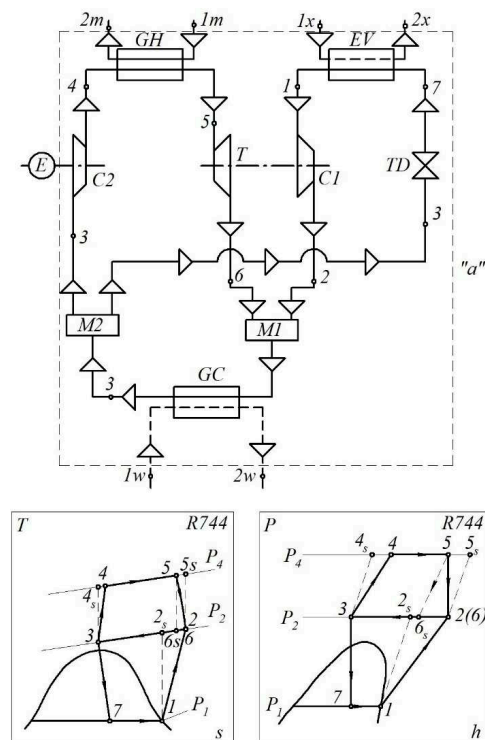


Figure 1. The initial design scheme (contour “a”) and working cycle of an R744 heat-using transformer: GH—gas heater; GC—gas cooler; EV—evaporator; C1, C2—compressors; T—turbine; E—engine; TD—throttling device; M1, M2—collectors; 1–7—the working substance of the circulation circuit; 1m, 2m—heating medium; 1x, 2x—coolant; 1w, 2w—consumer coolant or cooling tower.

In the basic scheme (Figure 1), during the process 1–2 in compressor C1, CO₂ vapor is compressed after the evaporator to the intermediate pressure p_2 of the cycle. The operation of compressor C1 is realized due to the transfer of mechanical work generated in the gas turbine T during the expansion of CO₂ from the state at point 5 to the state at point 6. Simultaneously, the conditions $p_6 = p_2$ and, consequently, $t_6 = t_2$ are supported.

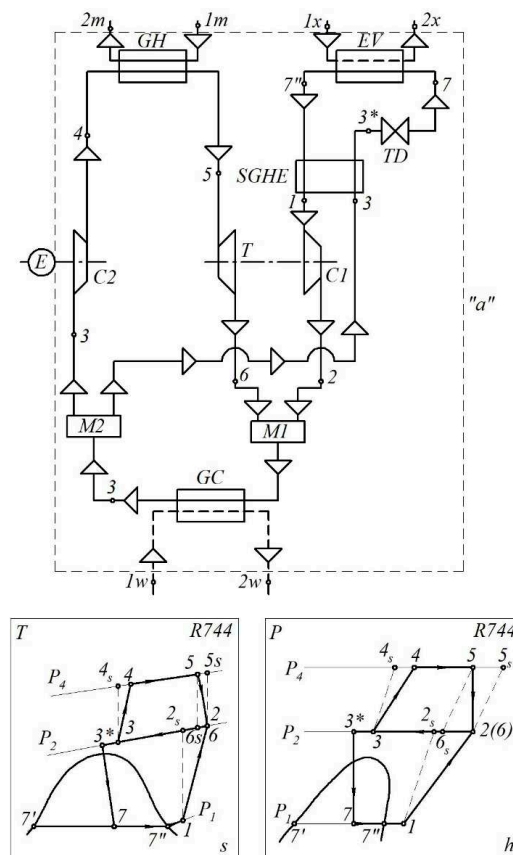


Figure 2. The initial design scheme (contour “a”) and working cycle of an R744 heat-using transformer with an SGHE: GH—gas heater; GC—gas cooler; EV—evaporator; C1, C2—compressors; T—turbine; E—engine; TD—throttling device; M1, M2—collectors; 1–7—the working substance of the circulation circuit; 1m, 2m—heating medium; 1x, 2x—coolant; 1w, 2w—consumer coolant or cooling tower.

Next, in the gas cooler GC, the carbon dioxide mixture after the turbine and compressor C1 is cooled to the state at point 3 (process 2–3). This process is implemented due to the heat exchange between carbon dioxide and the heating medium:

- In the heat pump mode—the heating of the coolant for the consumer of the heat load (e.g., heating, hot water supply, and so on);
- In the cooling mode—the discharge of heat in the process 2–3 into the environment or deeper energy utilization.

After the gas cooler, the flow of CO₂ with the parameters at point 3 is divided into two parts. Part *M* (from the total mass flow through the gas cooler) is returned through the throttle device to the evaporator and then to compressor C1, and part (1 – *M*) goes to compressor C2 for compression.

In compressor C2, carbon dioxide is compressed to pressure p_4 and acquires the state parameters at point 4. Compression is provided due to the introduction of mechanical work from an external engine. A further increase in the energy of the CO₂ gas flow for the turbine (state of point 5) is realized in the gas heater GH by supplying heat from the flow of the external coolant (of any generation or aggregate state): $\dot{Q}_{4-5} = \dot{Q}_{1m-2m}$. The second part of the carbon dioxide after the gas cooler is throttled to the pressure in the evaporator (process 3–7). Evaporation of the CO₂ liquid phase (process 7–1) occurs due to the transfer of low-potential heat from an external source (manufactured or natural), depending on the operation mode of the thermotransformer: $\dot{Q}_{7-1} = \dot{Q}_{1x-2x}$. Overall, the total energy resource used for thermal transformation is hybrid. It consists of the energy of the drive motor for the compressor C2 and heat for heating CO₂ in the gas heater.

The main difference between the basic scheme (Figure 2) and the scheme presented in Figure 1 is that the CO₂ vapors in front of the C1 compressor are overheated by 5–20 °C due to heat in the SGHE. Simultaneously, carbon dioxide after the gas cooler is subcooled in the SGHE (process 3–3*). The installation of a regenerative heat exchanger in this scheme provides the following advantages of the cycle. Firstly, it allows higher temperature values, $t_2 = t_6$, to be obtained and, accordingly, higher heating temperatures of the external coolant for the heat pump operation mode. Secondly, due to the supercooling of the gas under intermediate pressure after throttling, it also allows saturated steam (state of point 7) with less dryness to be obtained and the heat load on the evaporator to be increased.

Therefore, the proposed design scheme is rational for the heat pump mode of operation of the thermotransformer.

2.2. The Calculation Model

Below, a calculation model for the initial and proposed design schemes is developed under certain assumptions. Firstly, the model assumes the equality of the parameters of the refrigerant when mixing after the turbine and compressor C1. In other words, the parameters at point 2 are equal to those at point 6. Secondly, the parameters at points 2s and 4s are determined under conditions of isentropic compression in compressors C1 and C2, respectively. Thirdly, the parameters at points 2 and 4 are determined under the conditions of polytropic compression in compressors C1 and C2, respectively.

Under these assumptions, the temperature at point 3 is determined as follows:

$$t_3 = t_{1x} + \Delta t_{ur}, \quad (1)$$

where Δt_{ur} is the under-recovery rate used to assess the energy efficiency of the design scheme.

Point 5s is a point that assumes the state of the refrigerant at the turbine inlet. It was introduced so that the final state in the refrigerant's isentropic expansion at 5s–6 was characterized by the parameters at point 6, which are equal to the parameters at point 2. This assumption is acceptable in the given interval of pressure changes, p_5 – p_2 .

Also, the inlet pressure in turbine T equals the outlet pressure from the gas heater GH ($p_4 = p_5$). It is determined as follows:

$$p_5 = \beta \cdot p_2, \quad (2)$$

where $\beta = 1.2$ – 1.8 is the pressure ratio for the compressor C2.

The throttling process is considered isoenthalpic. Therefore, $h_7 = h_3$, and other parameters at point 7 are determined under the condition $p_7 = p_{ev}$.

Within the intersection of external material and energy flows (Figure 1, contour "a"), the energy balance is as follows:

$$\dot{Q}_{GH} + \dot{Q}_{EV} + N_{e,C2} = \dot{Q}_{GC}; \quad (3)$$

$$G_T \cdot (h_{1T} - h_{2T}) + G_x \cdot (h_{1x} - h_{2x}) + N_{e,C2} = G_w \cdot (h_{2w} - h_{1w}). \quad (4)$$

The energy balance equation, Equation (3), from the side of the refrigerant takes the following form:

$$\dot{m}_{GH} \cdot (h_5 - h_4) + \dot{m}_{EV} \cdot (h_1 - h_7) + \dot{m}_{GH} \cdot l_{e,C2} = \dot{m}_{GC} \cdot (h_2 - h_3), \quad (5)$$

where $l_{e,C2} = (h_4 - h_3) / \eta_{mech,C2}$ is the specific effective work of the compressor C2.

The refrigerant mass flow rate balance is as follows:

$$\dot{m}_{GC} = \dot{m}_{GH} + \dot{m}_{EV}. \quad (6)$$

After considering the mass flow rate through the evaporator and, accordingly, through the compressor C1,

$$M = \frac{\dot{m}_{EV}}{\dot{m}_{GH}} = \frac{\dot{m}_{C1}}{\dot{m}_{GH}}, \quad (7)$$

the mass flow through the gas cooler takes the following form:

$$\dot{m}_{GC} = \dot{m}_{GH} \cdot (1 + M). \quad (8)$$

After equal transformations and considering that for the throttling process $h_7 = h_3$,

$$(h_5 - h_4) + M \cdot (h_1 - h_3) + \frac{h_4 - h_3}{\eta_{mech, C2}} = (1 + M) \cdot (h_2 - h_3); \quad (9)$$

$$(h_5 - h_4) + \frac{h_4 - h_3}{\eta_{mech, C2}} - (h_2 - h_3) = M \cdot (h_2 - h_1). \quad (10)$$

The ratio M becomes equal to

$$M = \frac{(h_5 - h_4) + \frac{h_4 - h_3}{\eta_{mech, C2}} - (h_2 - h_3)}{h_2 - h_1}; \quad (11)$$

$$M = \frac{\Delta q + l_{e,C2}}{l_{i,C2}}, \quad (12)$$

where $l_{i,C2} = h_2 - h_1$ is the specific work of the compressor $C1$; $\Delta q = q_{GH} - q_{GC} = (h_5 - h_4) - (h_2 - h_3)$.

Based on the heat load transferred to the gas cooler, the mass flow can be determined as follows:

$$\dot{m}_{GC} = \frac{\dot{Q}_V}{q_{GC}} = \frac{\dot{Q}_{GC}}{(h_2 - h_3)}. \quad (13)$$

Therefore,

$$\dot{m}_{GH} = \frac{\dot{m}_{GC}}{(1 + M)}; \quad (14)$$

$$\dot{m}_{EV} = \dot{m}_{C1} = \dot{m}_{GC} - \dot{m}_{GH} = \dot{m}_{GC} \cdot \frac{M}{(1 + M)}. \quad (15)$$

The energy efficiency of the working cycle is as follows:

$$COP_{TN} = \frac{\dot{Q}_{GC}}{\dot{Q}_{GH} + N_{e,C2}}; \quad (16)$$

$$COP_{TN} = \frac{\dot{m}_{GC} \cdot q_{GC}}{\dot{m}_{GH} \cdot q_{GH} + \dot{m}_{GH} \cdot l_{e,C2}}; \quad (17)$$

$$COP_{TN} = \frac{(1 + M) \cdot (h_2 - h_3)}{(h_5 - h_4) + \frac{h_4 - h_3}{\eta_{mech, C2}}} = \frac{(1 + M) \cdot q_{GC}}{q_{GH} + \frac{l_{e,C2}}{\eta_{mech, C2}}}. \quad (18)$$

Also, the cycle coefficient of performance for primary energy resources takes the following form:

$$COP_{\Sigma} = \frac{\dot{Q}_{GC}}{\frac{\dot{Q}_{GH}}{COP_{TG}} + \frac{N_{e,C2}}{COP_{EG}}}; \quad (19)$$

$$COP_{\Sigma} = \frac{(1 + M) \cdot (h_2 - h_3)}{\frac{h_5 - h_4}{COP_{TG}} + \frac{h_4 - h_3}{\eta_{mech, C2} \cdot COP_{EG}}} = \frac{(1 + M) \cdot q_{GC}}{\frac{q_{GH}}{COP_{TG}} + \frac{l_{e,C2}}{COP_{EG}}}, \quad (20)$$

where $COP_{TG} = 0.9$ and $COP_{EG} = 0.3$ are the energy efficiency of thermal and electricity generation, respectively.

For the design scheme presented in Figure 2, Equation (5) takes the following form:

$$\dot{m}_{GH} \cdot (h_5 - h_4) + \dot{m}_{EV} \cdot (h_{7''} - h_7) + \dot{m}_{GH} \cdot l_{e,C2} = \dot{m}_{GC} \cdot (h_2 - h_3), \dot{m}_{GC} = \frac{\dot{Q}_V}{q_{GC}} = \frac{\dot{Q}_{GC}}{(h_2 - h_3)}, \tag{21}$$

or after considering the ratio M :

$$(h_5 - h_4) + M \cdot (h_{7''} - h_{3^*}) + \frac{h_4 - h_3}{\eta_{mech, C2}} = (1 + M) \cdot (h_2 - h_3). \tag{22}$$

For the option with the SGHE, the balance equation is as follows:

$$h_1 - h_{7''} = h_3 - h_{3^*}, \tag{23}$$

Therefore, $h_{7''} - h_{3^*} = h_1 - h_3$, and Equation (21) completely repeats Equation (9). Moreover, Equations (10)–(20) can be applied to calculate this option.

2.3. The Proposed Design Schemes

The proposed design schemes and working cycles are presented in Figures 3 and 4. The functioning of thermotransformers, according to alternative schemes, involves switching the drive for the compressor C2 from the gas turbine T2. In this case, after the gas heater, the flow of CO₂ is divided into two turbines in proportion to the mechanical work required to drive compressors C1 and C2, respectively. The turbines operate in the same range of parameters (process 5–6). Due to the change in the energy supply to drive the compressor C2, the thermal load on the gas heater increases (due to the increase in the mass flow rate of both media in the heater). Such a scheme is more energy-effective when using resettable coolants. The operation of other system components is similar to the basic schemes shown in Figures 1 and 2.

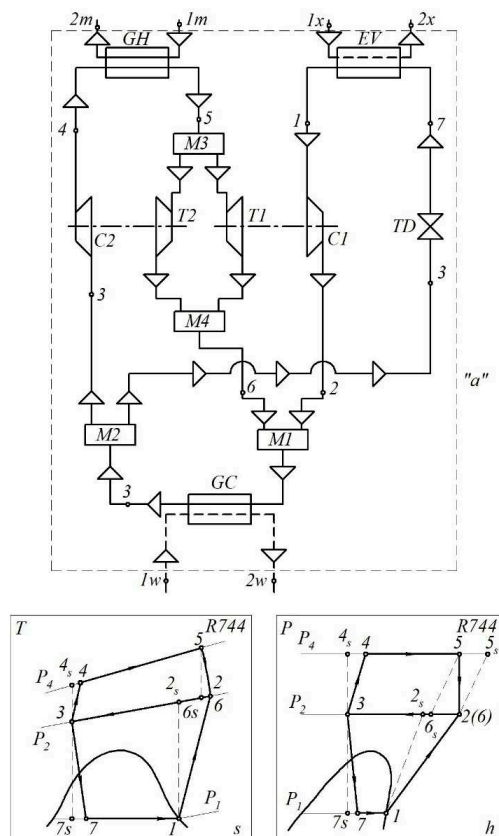


Figure 3. The proposed design scheme (contour “a”) and working cycle of an R744 heat-using thermotransformer with throttling in the reverse cycle circuit: GH—gas heater; GC—gas cooler; EV—evaporator; C1, C2—compressors; T1, T2—turbines; TD—throttling device; M1–M4—collectors; 1–7—the working substance of the circulation circuits; 1m, 2m—heating medium; 1x, 2x—coolant; 1w, 2w—consumer coolant or cooling tower.

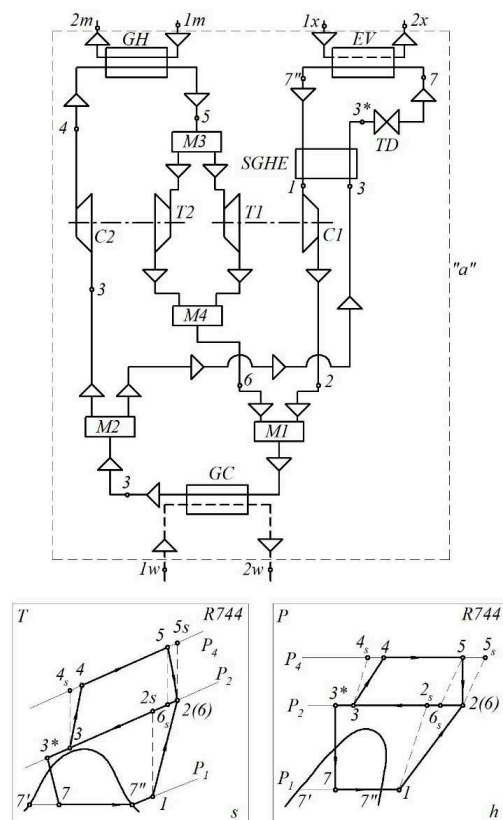


Figure 4. The proposed design scheme (contour “a”) and working cycle of an R744 heat-using thermo-transformer with an SGHE: GH—gas heater; GC—gas cooler; EV—evaporator; C1, C2—compressors; T1, T2—turbines; TD—throttling device; M1–M4—collectors; 1–7—the working substance of the circulation circuits; 1m, 2m—heating medium; 1x, 2x—coolant; 1w, 2w—consumer coolant or cooling tower.

2.4. The Calculation Model of the Proposed Design

The energy balance equation for the design scheme presented in Figure 3 within the contour “a”,

$$\dot{Q}_{GH} + \dot{Q}_{EV} = \dot{Q}_{GC} \tag{24}$$

has the following solution from the side of the refrigerant:

$$\dot{m}_{GH} \cdot (h_5 - h_4) + \dot{m}_{EV} \cdot (h_1 - h_3) = (\dot{m}_{GH} + \dot{m}_{EV}) \cdot (h_2 - h_3). \tag{25}$$

As for the initial design scheme, the ratio *M* of the mass flow rate through the evaporator is also considered:

$$M = \frac{\dot{m}_{EV}}{\dot{m}_{GH}} = \frac{\dot{m}_{C1}}{\dot{m}_{GH}}. \tag{26}$$

After an equal transform, this equation takes the following form:

$$(h_5 - h_4) + M \cdot (h_1 - h_3) = (1 + M) \cdot (h_2 - h_3); \tag{27}$$

$$(h_5 - h_4) - (h_2 - h_3) = M \cdot (h_2 - h_1). \tag{28}$$

Therefore, the ratio *M* takes the following form:

$$M = \frac{(h_5 - h_4) - (h_2 - h_3)}{h_2 - h_1}; \tag{29}$$

$$M = \frac{q_{GH} + q_{GC}}{l_{i,C1}}. \quad (30)$$

The mass flow rates, \dot{m}_{GH} , \dot{m}_{EV} , and \dot{m}_{GC} , are determined by the same equations, Equations (13)–(15), as for the initial design scheme. However, in contrast to the initial scheme, the mass flow rate of the refrigerant after the gas heater is divided into two flows that pass through the turbines $T1$ and $T2$ with parts Z and $(1 - Z)$, respectively.

Therefore, the following partial relations are introduced:

$$Z = \frac{\dot{m}_{T1}}{\dot{m}_{GH}}; \quad (31)$$

$$1 - Z = \frac{\dot{m}_{T2}}{\dot{m}_{GH}}. \quad (32)$$

Thus, for the design scheme presented in Figure 5, the following relations can be written:

$$\dot{m}_{GH} \cdot (h_4 - h_3) + (1 - Z) \cdot \dot{m}_{GH} \cdot (h_6 - h_5) = 0; \quad (33)$$

$$h_4 - h_3 = (1 - Z) \cdot (h_5 - h_6); \quad (34)$$

$$1 - Z = \frac{h_4 - h_3}{h_5 - h_6}; \quad (35)$$

$$Z = 1 - \frac{h_4 - h_3}{h_5 - h_6}. \quad (36)$$

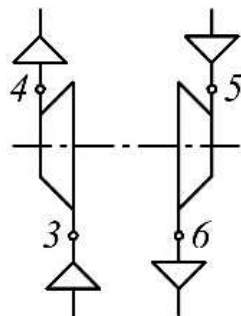


Figure 5. The design scheme of inlet and outlet flows.

Overall, the energy efficiency of the cycle in the heat pump mode is as follows:

$$COP_{TN} = COP_{\Sigma}; \quad (37)$$

$$COP_{TN} = \frac{\dot{Q}_W}{\dot{Q}_T} = \frac{\dot{Q}_{GC}}{\dot{Q}_{GH}}; \quad (38)$$

$$COP_{TN} = \frac{\dot{m}_{GC} \cdot (h_2 - h_3)}{\dot{m}_{GH} \cdot (h_5 - h_4)}; \quad (39)$$

$$COP_{TN} = (1 + M) \cdot \frac{q_{GC}}{q_{GH}}. \quad (40)$$

3. Results

The energy efficiency calculation results obtained for the initial and proposed design schemes are presented below.

Calculations were carried out for different operating modes of the thermotransformer depending on the pressure ratio between compressors C1 and C2. Table 1 shows the calculation of the mode parameters of the refrigerant R744 at the nodal points of the cycle for the basic scheme (Figure 1) and the proposed scheme (Figure 3). Table 2 shows the same for the basic scheme (Figure 2) and the proposed scheme (Figure 4).

Table 1. Parameters of the refrigerant R744 at the nodal points of the cycle for the basic scheme (Figure 1) and the proposed scheme (Figure 3).

$p_2 = 90 \text{ bar}; \beta = p_4/p_2 = 1.3; t_{ev} = 5 \text{ }^\circ\text{C}; t_3 = 45 \text{ }^\circ\text{C}$										
Parameter	1	2s	2	3	4s	4	5s	5	6	7
$t, \text{ }^\circ\text{C}$	5.0	68.0	72.1	45.0	61.7	62.1	94.2	93.3	72.1	5.0
$p, \text{ bar}$	39.7	90.0	90.0	90.0	117.0	117.0	117.0	117.0	90.0	39.7
$h, \text{ kJ/kg}$	427.8	459.1	466.9	387.5	394.8	396.6	479.0	477.2	466.9	387.5
$s, \text{ kJ/(kg}\cdot\text{K)}$	1817.3	1817.3	1840.1	1598.7	1598.7	1604.2	1840.1	1835.2	1840.1	–
$v, 10^{-6} \text{ m}^3/\text{kg}$	875.0	471.0	492.0	291.0	252.0	255.0	408.0	405.0	492.0	–
$p_2 = 100 \text{ bar}; \beta = p_4/p_2 = 1.3; t_{ev} = 5 \text{ }^\circ\text{C}; t_3 = 45 \text{ }^\circ\text{C}$										
Parameter	1	2s	2	3	4s	4	5s	5	6	7
$t, \text{ }^\circ\text{C}$	5.0	76.7	81.4	45.0	56.9	57.2	103.8	102.8	81.4	5.0
$p, \text{ bar}$	39.7	100.0	100.0	100.0	130.0	130.0	130.0	130.0	100.0	39.7
$h, \text{ kJ/kg}$	427.8	463.6	472.6	347.7	353.5	354.9	485.1	483.2	472.6	347.7
$s, \text{ kJ/(kg}\cdot\text{K)}$	1817.3	1817.3	1842.8	1466.0	1466.0	1470.4	1842.8	1837.8	1842.8	–
$v, 10^{-6} \text{ m}^3/\text{kg}$	875.0	437.0	458.0	201.0	184.0	185.0	382.0	378.0	458.0	–
$p_2 = 120 \text{ bar}; \beta = p_4/p_2 = 1.3; t_{ev} = 5 \text{ }^\circ\text{C}; t_3 = 45 \text{ }^\circ\text{C}$										
Parameter	1	2s	2	3	4s	4	5s	5	6	7
$t, \text{ }^\circ\text{C}$	5.0	92.0	97.8	45.0	59.0	53.5	120.7	119.6	97.8	5.0
$p, \text{ bar}$	39.7	120.0	120.0	120.0	156.0	156.0	156.0	156.0	120.0	39.7
$h, \text{ kJ/kg}$	427.8	471.8	482.8	314.6	319.9	321.3	496.2	494.2	482.8	314.6
$s, \text{ kJ/(kg}\cdot\text{K)}$	1817.3	1817.3	1847.2	1351.2	1351.2	1355.3	1847.2	1842.2	1847.2	–
$v, 10^{-6} \text{ m}^3/\text{kg}$	875.0	385.0	406.0	153.0	146.0	147.0	341.0	338.0	406.0	–

Table 2. Parameters of the refrigerant R744 at the nodal points of the cycle for the basic scheme (Figure 2) and the proposed scheme (Figure 4).

$p_2 = 90 \text{ bar}; \beta = p_4/p_2 = 1.2; t_{ev} = 5 \text{ }^\circ\text{C}; t_1 = 10 \text{ }^\circ\text{C}; t_3 = 45 \text{ }^\circ\text{C}$												
Parameter	1	2s	2	7''	3	3*	4s	4	5s	5	6	7
$t, \text{ }^\circ\text{C}$	10.0	74.0	78.8	5.0	45.0	43.6	56.6	56.9	94.4	93.7	78.8	5.0
$p, \text{ bar}$	39.7	90.0	90.0	39.7	90.0	90.0	108.0	108.0	108.0	108.0	90.0	39.7
$h, \text{ kJ/kg}$	437.0	470.5	478.8	427.8	387.5	378.2	392.5	393.7	487.7	486.3	478.8	378.2
$s, \text{ kJ/(kg}\cdot\text{K)}$	1850.4	1850.4	1874.3	1817.3	1598.7	1569.5	1598.7	1602.5	1874.3	1870.7	1874.3	1639.3
$v, 10^{-6} \text{ m}^3/\text{kg}$	935.0	501.0	524.0	875.0	291.0	271.0	263.0	265.0	459.0	456.0	524.0	699.5
$p_2 = 90 \text{ bar}; \beta = p_4/p_2 = 1.2; t_{ev} = 5 \text{ }^\circ\text{C}; t_1 = 15 \text{ }^\circ\text{C}; t_3 = 45 \text{ }^\circ\text{C}$												
Parameter	1	2s	2	7''	3	3*	4s	4	5s	5	6	7
$t, \text{ }^\circ\text{C}$	15.0	79.9	85.3	5.0	45.0	42.6	56.6	56.9	101.1	100.3	85.3	5.0
$p, \text{ bar}$	39.7	90.0	90.0	39.7	90.0	90.0	108.0	108.0	108.0	108.0	90.0	39.7
$h, \text{ kJ/kg}$	445.3	480.7	489.5	427.8	387.5	369.9	392.5	393.7	498.8	497.4	489.5	369.9
$s, \text{ kJ/(kg}\cdot\text{K)}$	1879.4	1879.4	1904.3	1817.3	1598.7	1543.3	1598.7	1602.5	1904.3	1900.6	1904.3	–
$v, 10^{-6} \text{ m}^3/\text{kg}$	988.0	528.0	552.0	875.0	291.0	254.0	263.0	265.0	483.0	480.0	552.0	–

Table 2. Cont.

Parameter	$p_2 = 90 \text{ bar}; \beta = p_4/p_2 = 1,2; t_{ev} = 5 \text{ }^\circ\text{C}; t_1 = 20 \text{ }^\circ\text{C}; t_3 = 45 \text{ }^\circ\text{C}$											
	1	2s	2	7"	3	3*	4s	4	5s	5	6	7
$t, \text{ }^\circ\text{C}$	15.0	85.6	91.6	5.0	45.0	41.8	56.6	56.9	107.7	106.7	91.6	5.0
$p, \text{ bar}$	39.7	90.0	90.0	39.7	90.0	90.0	108.0	108.0	108.0	108.0	90.0	39.7
$h, \text{ kJ/kg}$	453.0	490.0	499.3	427.8	387.5	362.3	392.5	393.7	509.0	507.5	499.3	362.3
$s, \text{ kJ/(kg}\cdot\text{K)}$	1905.7	1905.7	1931.3	1817.3	1598.7	1519.0	1598.7	1602.5	1931.3	1927.4	1931.3	–
$v, 10^{-6} \text{ m}^3/\text{kg}$	1037.0	553.0	578.0	875.0	291.0	239.0	263.0	265.0	505.0	502.0	578.0	–

The results are given for one mode of operation; however, there are about 50 operating modes.

Figure 6 shows the cycle coefficient of the performance calculation results for the initial design scheme presented in Figure 1.

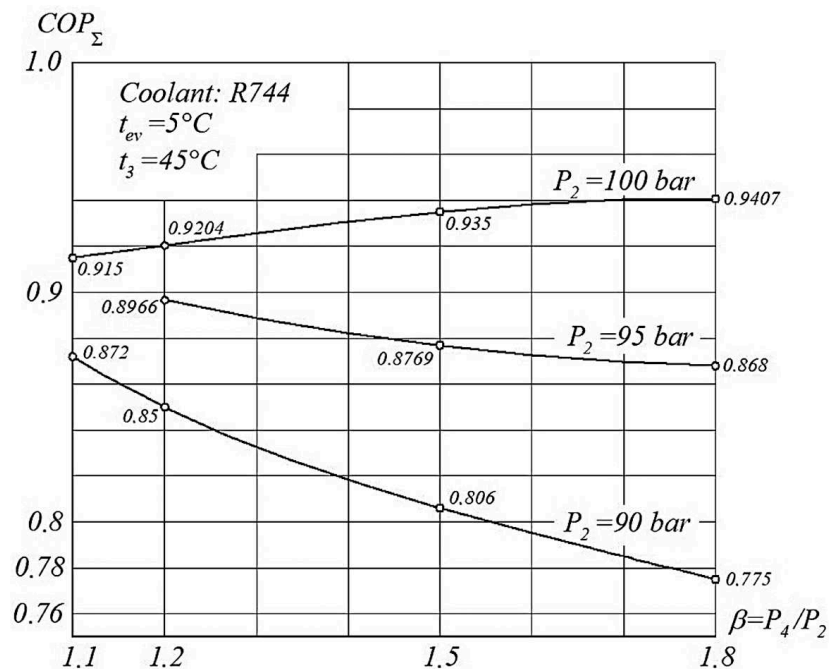


Figure 6. The cycle coefficient of performance calculation results for the initial design scheme shown in Figure 1.

Figure 6 shows that at the same value of the pressure ratio $\beta = p_4/p_2$, but at different values of the pressure p_2 at the inlet to the compressor C1, the value of the cycle conversion factor will be different. Particularly, for $\beta = 1.2$, the efficiency of the cycle will be greatest at a pressure value of $p_2 = 100 \text{ bar}$. The same will be observed with an increase in the pressure rate β .

Simultaneously, if the pressure ratio in compressor C2 is increased, at the pressure values of $p_2 = 90 \text{ bar}$ and $p_2 = 95 \text{ bar}$ at the outlet of compressor C1, the value of η_Σ will decrease for a certain pressure value p_2 . Overall, the cycle coefficient of the performance for the initial design scheme is $\eta_\Sigma = 0.775 - 0.941$.

Figure 7 presents the calculation results of the cycle coefficient of the performance for the proposed scheme presented in Figure 3.

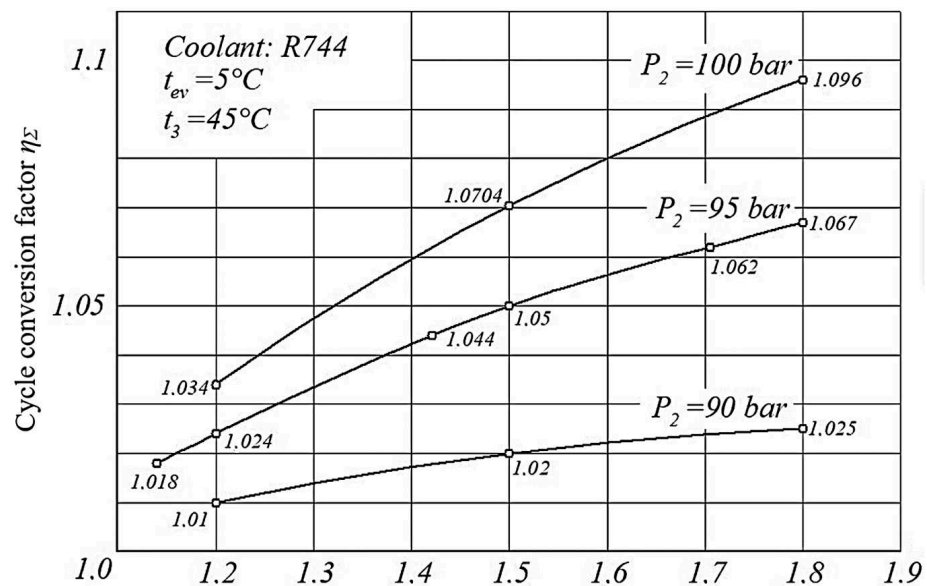


Figure 7. The cycle coefficient of performance calculation results for the proposed design scheme, shown in Figure 3.

Figure 7 shows that for the proposed scheme, as well as for the basic one, at the same value of the pressure ratio $\beta = p_4/p_2$, but at different values of the pressure p_2 at the input to the compressor C1, the value of the cycle conversion factor will be different. However, the main difference is that with an increase in the pressure p_2 at the outlet of the compressor C1, the value of the conversion factor of the cycle constantly increases in the range of $\beta = 1.2$ –1.8. Overall, the cycle coefficient of the performance for the initial design scheme is $\eta_{\Sigma} = 1.010$ –1.096.

After analyzing the results presented in Figure 6 for the basic scheme and Figure 7 for the proposed scheme, it can be concluded that using a new heat-using scheme makes it possible to increase the conversion factor of the cycle by an average of 18.5%.

Moreover, an interesting feature of the curves presented in Figures 6 and 7 is that an increase in the pressure ratio in the compressor C2 leads to an increase in the cycle coefficient of the performance, COP_{Σ} .

Figure 8 presents the proposed design scheme's cycle coefficient of the performance calculation results for the pressure ratio $\beta = 1.1$ –5.0 in the compressor C2.

Figure 8 shows that with an increase in the degree of the pressure ratio in a range of $\beta = 2.0$ –5.0, the curves of the cycle conversion factor for the pressure $p_2 = 90$ bar reach the extremum at $\beta = 2.2$, and for $p_2 = 100$ bar at $\beta = 4.0$. Therefore, the most significant values of the cycle conversion coefficients for $p_2 = 90$ bar will be in the interval $\beta = 1.8$ –2.5, and for $p_2 = 100$ bar at $\beta = 3$ –5.

For the value of the suction pressure in the compressor C1 near $p_2 = 110$ bar, the curve of the values of the conversion coefficients of the cycle will have a constantly increasing character. Therefore, the highest efficiency ratio will be in the range of $\beta = 4$ –5.

Another energy efficiency indicator is the dependence of the cycle coefficient of performance, η_{Σ} , on the suction temperature, t_1 , in the compressor C1 (Figure 9).

From Figure 9, an increase in the suction temperature of the compressor C1 increases the energy efficiency of the proposed design scheme of the R744 heat-using thermotransformer. Therefore, the most significant cycle coefficient of the performance is reached at $t_1 = 25$ –30 °C.

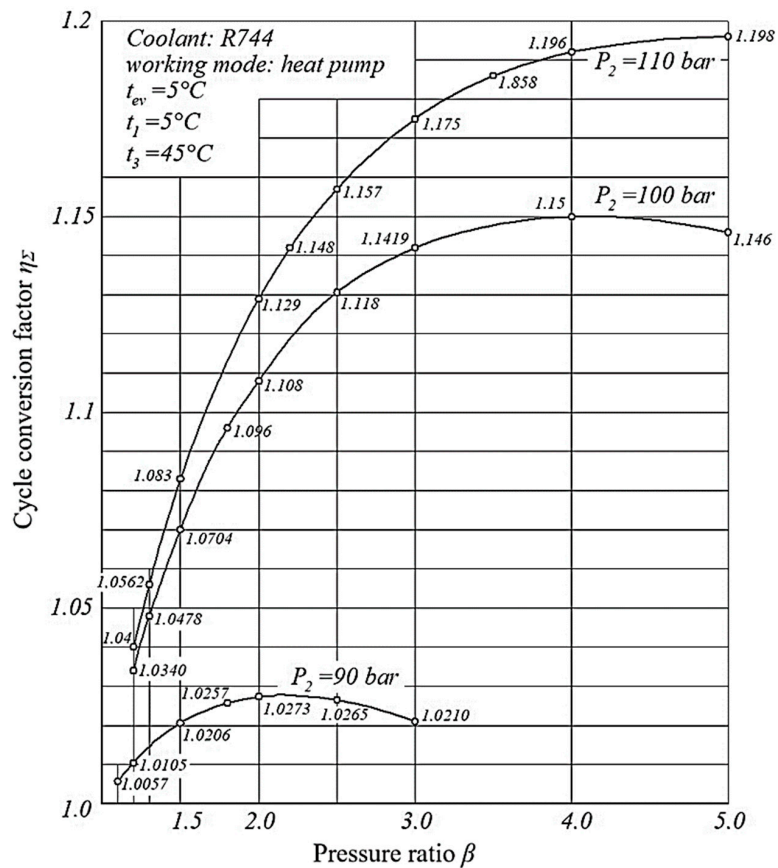


Figure 8. The cycle coefficient of performance calculation results for the proposed design scheme of an R744 heat-using thermotransformer for the pressure ratio $\beta = 1.1\text{--}5.0$ in compressor C2.

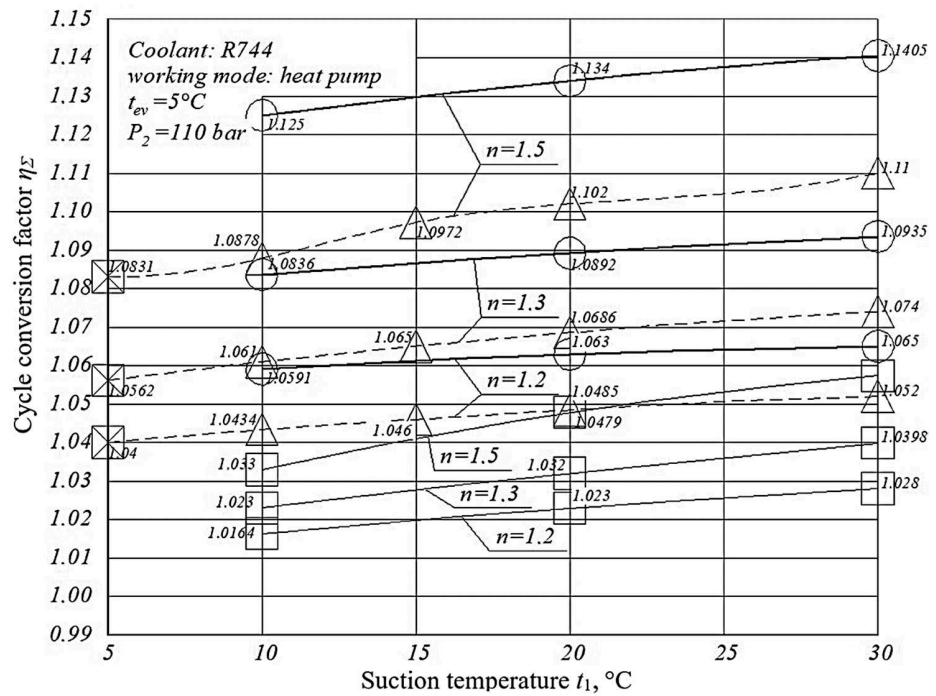


Figure 9. The dependence of the cycle coefficient of performance on the suction temperature in compressor C1 for the proposed design scheme of an R744 heat-using thermotransformer: ○— $t_3 = 35\text{ }^\circ\text{C}$; △— $t_3 = 45\text{ }^\circ\text{C}$; □— $t_3 = 55\text{ }^\circ\text{C}$; ⊠— $t_1 = t_{ev} = 5\text{ }^\circ\text{C}$.

4. Discussion

Thus, after analyzing the results obtained in Section 2 and evaluating the numerical calculation results for the initial and proposed design schemes presented in Figures 1–4, it is possible to determine a number of advantages of using the proposed design schemes with a throttling device (Figure 3) and an SGHE (Figure 4). The primary advantage is the rejection of the drive motor, which is necessary to drive the compressor C2 in the initial design schemes.

Also, in the proposed design schemes, the equality of the capacities of the compressor C1 and the turbine T1, located on a joint shaft, is ensured due to regulating mass flow rates in these devices. The cycle coefficient of performance is also increased for the proposed design scheme compared to the previous research results [7–11].

The results obtained in Section 3 show that the energy efficiency of the proposed design schemes is higher than that of the initial ones. It is increased with an increase in the pressure ratio in the compressor. Also, the efficiency of the proposed design schemes is increased by an increase in this ratio and the suction pressure in the compressor. This is explained by separating the mass flow of the refrigerant after the gas heater into two flows that pass through the turbines T1 and T2.

When creating a calculation model, as presented in Section 2, the given assumptions can be considered a research limitation. They do not significantly affect the accuracy of the obtained results, although their reduction significantly complicates the proposed model. Nevertheless, the results' reliability is proven by the relative calculation error, which does not exceed 5%. This value is sufficient for the evaluation of energy efficiency indicators.

Overall, this research presents the numerical calculation results for heat-using thermotransformers according to the proposed design model. The novelty of this article is the development of a model for evaluating the efficiency of thermotransformers.

A comparison with the experimental studies for existing analogs [12–17] at different operation modes and refrigerants will be carried out in further studies. Finding an optimal value of the pressure ratio between compressors C1 and C2 is also one of the next stages.

5. Conclusions

As a result of the analysis of existing heat-using thermotransformers, the two most effective design schemes were determined. The first is a design scheme with a throttling device, and the second is a suction gas heat exchanger (SGHE), which operates as an evaporator. These schemes have a cycle coefficient of performance of 0.775–0.941. However, using an SGHE before the compressor enables an overheating of the refrigerant at the inlet of the compressor.

Heat recovery units were proposed to increase the energy efficiency of the initial design schemes. Due to the proposed design solutions, they allowed for the abandonment of the use of an external engine to drive the compressor. This made it possible to reduce electrical energy consumption and spend it on starting the turbine only. As a result of using new heat utilization schemes, the conversion factor of the cycle has increased up to 1.010–1.096.

A calculation model was developed to determine the thermodynamic and mode parameters of the cycle for a heat-using thermotransformer with the refrigerant R744 operating at the heat pump mode. Additionally, a calculation model was developed to evaluate the proposed cycle's energy efficiency indicators and assess the expediency of implementing the proposed design scheme. As a result, it was shown that using the proposed heat utilization schemes allows the cycle coefficient of performance to be increased by an average of 18.5%.

An analysis of the obtained energy efficiency indicators showed that implementing the proposed design scheme allows the energy efficiency of heat-using thermotransformers to be increased by an average of 23%, depending on the suction pressure in the compressor.

Author Contributions: Conceptualization, V.A. and S.S.; methodology, V.A., O.K. and S.S.; software, J.P., J.M. and I.P.; validation, J.M., I.P. and V.I.; formal analysis, O.K. and V.I.; investigation, V.A., J.P., O.K., S.S., J.M., I.P. and V.I.; resources, J.P. and J.M.; data curation, J.M. and V.I.; writing—original draft preparation, V.A., O.K. and S.S.; writing—review and editing, J.P., I.P. and V.I.; visualization, O.K. and S.S.; supervision, V.A.; project administration, I.P.; funding acquisition, J.P. All authors have read and agreed to the published version of the manuscript.

Funding: The research was partially funded by the project VEGA 1/0704/22, granted by the Ministry of Education, Science, Research and Sport of the Slovak Republic.

Data Availability Statement: The data presented in this study are available on request from the corresponding author.

Acknowledgments: The research was realized within the Ulam NAWA Programme, grant number BPN/U LM/2022/1/00042.

Conflicts of Interest: The authors declare no conflict of interest.

References

1. Malavika, S.; Chiranjeevi, C.; Sekhar, Y.R.; Srinivas, T.; Natarajan, M.; Myo, W.P.P.; Singh, A. Performance optimization of a heat pump for high temperature application. *Mater. Today Proc.* **2021**, *46*, 5278–5285. [\[CrossRef\]](#)
2. Wang, Z.; Li, G.; Wang, F.; Li, K.; Lou, Y. Techno-economic evaluation of a frost-free air source heat pump water heater. *Sustain. Cities Soc.* **2020**, *57*, 102102. [\[CrossRef\]](#)
3. Triebs, M.S.; Tsatsaronis, G. From heat demand to heat supply: How to obtain more accurate feed-in time series for district heating systems. *Appl. Energy* **2022**, *311*, 118571. [\[CrossRef\]](#)
4. Plotkin, J.; Levchenko, N.; Shyshkanova, G.; Levchenko, S. Development of energy enterprises in the context of green transformation. *J. Eng. Sci.* **2023**, *10*, G22–G33. [\[CrossRef\]](#)
5. Lorentzen, G. The use of natural refrigerants: A complete solution to the CFC/HCFC predicament. *Int. J. Refrig.* **1995**, *18*, 190–197. [\[CrossRef\]](#)
6. Sharapov, S.O.; Bocko, J.; Yevtushenko, S.O.; Panchenko, V.O.; Skydanenko, M.S. Energy-saving individual heating systems based on liquid-vapor ejector. *J. Eng. Sci.* **2023**, *10*, G1–G8. [\[CrossRef\]](#)
7. Lorentzen, G. Revival of carbon dioxide as a refrigerant. *Int. J. Refrig.* **1994**, *17*, 292–301. [\[CrossRef\]](#)
8. Gilani, B.S.; Morosuk, T. Improving the operation of heat exchanger networks through exergy analysis. *Int. J. Exergy* **2022**, *38*, 202. [\[CrossRef\]](#)
9. Topal, H.I.; Tol, H.I.; Kopaç, M.; Arabkoohsar, A. Energy, exergy and economic investigation of operating temperature impacts on district heating systems: Transition from high to low-temperature networks. *Energy* **2022**, *251*, 123845. [\[CrossRef\]](#)
10. Ghorbani, B.; Miansari, M.; Zendejboudi, S.; Hamedi, M.H. Exergetic and economic evaluation of carbon dioxide liquefaction process in a hybridized system of water desalination, power generation, and liquefied natural gas regasification. *Energy Convers. Manag.* **2020**, *205*, 112374. [\[CrossRef\]](#)
11. Huang, C.; Li, Z.; Ye, Z.; Wang, R. Thermodynamic study of carbon dioxide transcritical refrigeration cycle with dedicated subcooling and cascade recooling. *Int. J. Refrig.* **2022**, *137*, 80–90. [\[CrossRef\]](#)
12. Liu, J.; Zhou, L.; Cheng, J.; Lin, Z.; Zhang, X. A novel two-stage compression air-source heat pump cycle combining space heating, cooling, and domestic hot water production. *Energy Build.* **2023**, *285*, 112863. [\[CrossRef\]](#)
13. Ahmadi, P.; Dincer, I.; Rosen, M.A. Thermodynamic modeling and multi-objective evolutionary-based optimization of a new multigeneration energy system. *Energy Convers. Manag.* **2013**, *76*, 282–300. [\[CrossRef\]](#)
14. DinAli, M.N.; Ibrahim, D. Development and analysis of an integrated gas turbine system with compressed air energy storage for load leveling and energy management. *Energy* **2018**, *163*, 604–617. [\[CrossRef\]](#)
15. Manesh, M.H.K.; Onishi, V.C. Energy, exergy, and thermo-economic analysis of renewable energy-driven polygeneration systems for sustainable desalination. *Processes* **2021**, *9*, 210. [\[CrossRef\]](#)
16. Wu, L.; Xiao, S.; Hu, Y. Scheduling of the combined power and desalination system. *Chem. Eng. Trans.* **2020**, *81*, 1201–1206. [\[CrossRef\]](#)
17. Dai, B.; Qi, H.; Liu, S.; Ma, M.; Zhong, Z.; Li, J.; Song, M.; Sun, Z. Evaluation of transcritical CO₂ heat pump system integrated with mechanical subcooling by utilizing energy, exergy and economic methodologies for residential heating. *Energy Convers. Manag.* **2019**, *192*, 202–220. [\[CrossRef\]](#)
18. Xu, B.; Wang, X.; Zhang, Y.; Chen, Z. Experimental and economic analysis of optimization potential for annual operating characteristics of air source transcritical CO₂ heat pump system. *Therm. Sci. Eng. Prog.* **2023**, *42*, 101864. [\[CrossRef\]](#)
19. Dai, B.; Liu, S.; Sun, Z.; Ma, Y. Thermodynamic performance analysis of CO₂ transcritical refrigeration cycle assisted with mechanical subcooling. *Energy Procedia* **2017**, *105*, 2033–2038. [\[CrossRef\]](#)
20. Sharma, D.K.; Pegallapati, A.S.; Ramgopal, M. Performance of a CO₂ based transcritical air conditioning system under summer and winter conditions. *Therm. Sci. Eng. Prog.* **2023**, *41*, 101847. [\[CrossRef\]](#)

21. Li, R.; Ye, F.; Zhang, J.; Wang, M.; Li, K. Theoretical analysis of three CO₂/C₃H₈ (R744-R290) cascade refrigeration systems with precooling processes in low-temperature circuits. *Appl. Therm. Eng.* **2023**, *234*, 121238. [[CrossRef](#)]
22. Huang, H. *Heat Pumps for Cold Climate Heating*; CRC Press: Boca Raton, FL, USA, 2020; Volume 378. [[CrossRef](#)]
23. Llopis, R.; Cabello, R.; Sánchez, D.; Torrella, E. Energy improvements of CO₂ transcritical refrigeration cycles using dedicated mechanical subcooling. *Int. J. Refrig.* **2015**, *55*, 129–141. [[CrossRef](#)]
24. Llopis, R.; Nebot-Andrés, L.; Cabello, R.; Sánchez, D.; Catalán-Gil, J. Experimental evaluation of a CO₂ transcritical refrigeration plant with dedicated mechanical subcooling. *Int. J. Refrig.* **2016**, *69*, 361–368. [[CrossRef](#)]
25. Lazzaretto, A.; Tsatsaronis, G. SPECO: A systematic and general methodology for calculating efficiencies and costs in thermal systems. *Energy* **2006**, *31*, 1257–1289. [[CrossRef](#)]
26. Chen, F.; Morosuk, T. Exergetic and economic evaluation of CO₂ liquefaction processes. *Energies* **2021**, *14*, 7174. [[CrossRef](#)]
27. Morosuk, T.; Tsatsaronis, G. Advanced exergetic evaluation of refrigeration machines using different working fluids. *Energy* **2009**, *34*, 2248–2258. [[CrossRef](#)]

Disclaimer/Publisher’s Note: The statements, opinions and data contained in all publications are solely those of the individual author(s) and contributor(s) and not of MDPI and/or the editor(s). MDPI and/or the editor(s) disclaim responsibility for any injury to people or property resulting from any ideas, methods, instructions or products referred to in the content.